On the Thermodynamics, the Role of the Carbon Cathode, and the Cycle Life of the Sodium Superoxide (NaO2) Battery

ARTICLE *in* ADVANCED ENERGY MATERIALS · AUGUST 2014

Impact Factor: 16.15 · DOI: 10.1002/aenm.201301863

5 AUTHORS, INCLUDING:

Conrad Ludwig Bender
Justus-Liebig-Universität Gießen
10 PUBLICATIONS **180** CITATIONS

SEE PROFILE

P. Adelhelm
Friedrich Schiller University Jena
52 PUBLICATIONS **1,939** CITATIONS

SEE PROFILE

ADVANCED ENERGY MATERIALS
www.advenergymat.de

On the Thermodynamics, the Role of the Carbon Cathode, and the Cycle Life of the Sodium Superoxide (NaO_2) Battery

Conrad L. Bender, Pascal Hartmann, Miloš Vračar, Philipp Adelhelm, and Jürgen Janek**

Batteries based on the cell reaction between alkali metals and oxygen are highly attractive for energy storage due to their superior theoretical energy density. However, despite continuous progress, fundamental challenges in the further development of these cell systems remain. Understanding the oxygen electrode reaction and improving cycle life, while at the same time maximizing the practical energy density, are some of the most important issues that need to be addressed. Here, the product formation in aprotic sodium-oxygen cells is studied and it is shown how cycle life and practical capacities can be improved. Different cell reactions (leading to either NaO_2 or Na_2O_2 as discharge products) have recently been reported. To understand whether the carbon structure or the local current density has any influence on the product stoichiometry or the cell performance, several carbon materials with a broad range in properties are tested. Phase-pure NaO_2 is always found as a discharge product, but capacities range from 300 to values as high as 4000 mAh $g(C)^{-1}$ depending on the type of carbon. More importantly, the cycle life of Na/O_2 cells can be largely improved by shallow cycling, steadily yielding capacities of 1666 mAh $g(C)^{-1}$ for at least 60 cycles using a Ketjen black carbon electrode.

1. Introduction

In order to meet the future demand for electrochemical storage devices, safe batteries of lower cost and higher energy densities compared to established lithium ion technology are needed. The limitation in energy density of current lithium ion batteries (LIB) is rooted in the comparably high mass of the active components such as $LiCoO_2$, and the limited amount of lithium that can be reversibly stored per formula unit. In addition, the electrode materials are important cost factors. A possible alternative battery concept is based on the alkali metal-oxygen cell.[1] Here an alkali metal reacts at room temperature with atmospheric oxygen to form an oxide. Lithium for example can theoretically form Li_2O (not observed), Li_2O_2 (experimentally proven),[2–4] LiO_2 (as metastable intermediate) in non-aqueous electrolytes,[2] or LiOH in aqueous electrolytes[5–7] as possible discharge products. The key advantage of the alkali metal-oxygen cell is the high theoretical energy density, which by far exceeds the one of current lithium-ion technology.[8] Within the last years, most research was directed toward room-temperature lithium-oxygen cells with aprotic organic electrolytes that have been described first by Abraham et al. and for which Li_2O_2 has been found as major discharge product.[9] The theoretical gravimetric energy density w_{th} depends on the kind of discharge product and whether the mass of oxygen is included or not. The values for the formation of Li_2O_2 are 3456 Wh kg^{-1} based on the mass of the discharge product and 11 422 Wh kg^{-1} excluding the mass of the oxygen.[10] For comparison, a typical lithium ion battery based on graphite as negative and $LiCoO_2$ as positive electrode delivers 375 Wh kg^{-1} theoretically and today up to ≈200 Wh kg^{-1} practically.[11] Utilizing atmospheric oxygen might help to reduce cost even though the need for a conductive matrix that accommodates the discharge product (usually carbon) will counteract this benefit to some degree. Also the need for a filter system for oxygen has to be taken into account, as nitrogen, water and carbon dioxide interfere negatively with the cathode reaction. On the other hand, estimates on price and energy density of practical devices are still quite speculative as no functional demonstrator could be developed so far and several scientific and technological challenges remain. Still on the level of fundamental research, the current and most important tasks are 1) to understand and to minimize undesired side reactions between reduced oxygen species and cell components (electrolyte, electrodes) in order to achieve a sufficient cycle life,

C. L. Bender, Dr. P. Hartmann,
Dr. P. Adelhelm, Dr. J. Janek
Physikalisch-Chemisches Institut
Justus-Liebig-Universität Gießen
Heinrich-Buff-Ring 58, 35392 Gießen, Germany
E-mail: philipp.adelhelm@phys.chemie.uni-giessen.de;
juergen.janek@phys.chemie.uni-giessen.de
Dr. M. Vračar
Battery and Electrochemistry Laboratory (BELLA)
Institute of Nanotechnology, Karlsruhe Institute of Technology
Hermann-von-Helmholtz-Platz 1, 76344 Eggenstein-Leopoldshafen, Germany

DOI: 10.1002/aenm.201301863

2) to reduce the large overpotentials that are observed especially during charging (oxygen evolution reaction, OER), and 3) to understand the growth and decomposition mechanisms of the discharge product. Much effort is spent for the search of a suitable electrolyte, but up to now all solvents such as carbonates, ethers, dimethyl formamide and sulfones show signs of decomposition.[12–25] For the positive electrode, TiC has been recently proposed[26] as alternative to carbon based cathode materials that are unstable, particularly at potentials above 3.5 V that are needed for cell charge.[27] But even once the cathode issues are solved, the use of a pure metal anode necessitates measures against dendrite formation and continuous electrolyte reduction.

Beside lithium-oxygen cells there is also emerging interest in sodium-oxygen cells for reasons explained below, but research on Na/O_2 cells is still in an infant stage. However, the first publications showed that the reversibility of sodium-oxygen cells is much higher and also the overpotentials are much smaller compared to lithium cells. Another advantage of sodium over lithium is its unlimited resources.

Unlike for non-aqueous lithium-oxygen cells where Li_2O_2 is formed, reports on the nature of the discharge product in sodium-oxygen cells are less consistent and different discharge products have been reported. In early work Peled et al. assumed sodium peroxide as product but no experimental proof was given.[28] The cell operated at elevated temperatures using liquid sodium metal as negative electrode, which differs from later studies that aimed for room temperature operation. Liu et al. found polycrystalline Na_2O_2 as the discharge product using $NaPF_6$ or $NaClO_4$ in DME as electrolyte and taking selected area electron diffraction (SAED) as proof.[29] Sun et al. also found the peroxide but with a significant fraction of sodium carbonate using $NaPF_6$ in EC:DME 1:1 as electrolyte.[30] As proof they used results from SAED and FTIR spectroscopy. In a work by Kim et al. using a PC based electrolyte solution (1 M $NaClO_4$) sodium carbonate was the main discharge product, which was identified by X-ray diffraction and Fourier transform infrared (FTIR) spectroscopy.[31] In experiments using tetraglyme with 1 M $NaClO_4$ they found sodium peroxide dihydrate ($Na_2O_2 \cdot 2H_2O$) and trace amounts of sodium hydroxide by X-ray diffraction. They concluded that the discharge product depends on the electrolyte composition and proposed reaction mechanisms for both electrolyte compositions. Finally sodium peroxide was found by Das et al. when discharging the cell in an oxygen atmosphere, and sodium carbonate with some trace of oxalate was found when discharging the cell in an atmosphere consisting of a mixture of oxygen and carbon dioxide.[32] These products were identified using X-ray diffraction and FTIR spectroscopy. The used electrolyte was sodium perchlorate in tetraglyme.

In our own work (NaOTf in digylme) we found sodium superoxide as exclusive discharge product and proved its formation by X-ray diffraction, Raman spectroscopy and pressure monitoring during galvanostatic cycling.[33,34] As particular feature of the sodium superoxide cell we found that the discharge product crystallizes in form of large particles in the micrometer range enabling straight-forward studies on morphological properties by scanning electron microscopy (SEM), for example. Very recently the stability of the different product phases was calculated by two groups with somehow controversial results. Lee et al. conclude from first-principle calculations that NaO_2 and Li_2O_2 are the thermodynamically favored discharge products at standard conditions ($p(O_2) = 10^5$ Pa).[35] Also they showed that the equilibrium shape of the particles fits well to previously reported experimental data.[33,34] Kang et al. studied also the effect of particle size on the relative stability of Na_2O_2 and NaO_2.[36] In contradiction to Lee et al. they report that Na_2O_2 is the stable bulk phase at standard conditions, while NaO_2 can only become more stable at small particle sizes below 10 nm. The authors also conclude that NaO_2 nucleates much easier than the peroxide, suggesting kinetic control of the discharge product in non-aqueous Na/O_2 cells. Further work will be required to clear the discrepancies, but is obvious that the driving forces for formation of Na_2O_2 and NaO_2 are quite close.

Summarizing previous studies it can be stated so far that carbonate based electrolytes, as it is well known from lithium-oxygen cells, lead to severe side reactions involving Na_2CO_3 formation and to large overpotentials during charging. For ether based electrolytes, Na_2O_2, hydrated Na_2O_2 and NaO_2 have been identified as discharge products by different authors. Unfortunately, the experimental parameters are yet not known that allow steering between the reaction routes towards these different products. Obviously, the oxygen activity (i.e., the oxygen partial pressure) as major thermodynamic variable, controlling the chemical driving force, is not sufficient to explain the reported experimental observations. Otherwise the same discharge product should be observed by all authors at identical oxygen activity, which is not the case. Thus, kinetic control takes place, and various factors beyond the mere thermodynamic variables can influence the reaction route. In particular, the role of the carbon positive electrode (carbon type, surface area, morphology, surface chemistry) is highly ambiguous. Different carbon materials (carbon black, carbon fibers, graphene sheets, diamond-like carbon) have been used so far, making a direct comparison impossible. As we will show in the following, the thermodynamic driving forces for the formation of NaO_2 and Na_2O_2 are quite close, and other subtle effects may well decide on the formation of one or the other compound.

With respect to previous work on Na/O_2 cells the key question is: What determines the nature of the discharge product or how to reproducibly obtain only one of the products, i.e., the superoxide NaO_2 or the peroxide Na_2O_2 in a sodium-oxygen cell? The basic approach would be to vary the thermodynamic conditions such as oxygen partial pressure or temperature. As kinetic control of the discharge reaction appears to take place, the necessary approach is to systematically vary the reaction route, i.e., cell components such as the solvent mixture, type of conducting salt and type of positive electrode, gas purity or to change settings of the electrochemical measurement itself, e.g., applied current or potential windows.

Here, we first of all address the thermodynamic properties of the Na-O system in order to sketch out the free energy landscape of the competing reaction products and compare the results with the Li-O system. Secondly, we address the question whether the type of carbon being used as cathode has any influence on the product formation and the total capacity achievable. By using carbons with surface areas in the range between 1 $m^2\ g^{-1}$ and 1500 $m^2\ g^{-1}$ the resulting local current densi-

ties, based on the carbon surface area, range between 1.3 × 10^{-6} mA cm^{-2} up to 5.2 × 10^{-2} mA cm^{-2}, thus vary by more than four order of magnitude. Thirdly, as the cycle life of present sodium-oxygen cells has so far been comparably poor, we study how the capacity retention can be improved by changing the experimental conditions, i.e., cycling in a capacity limited mode (shallow cycling) instead of potential limited mode. In both cases, we try to provide a balanced view on the advantages and disadvantages that result from the variation in experimental conditions.

2. Results and Discussion

2.1. Thermodynamic Assessment of Sodium-Oxygen Cells

Metal-oxygen cells promise high specific capacities by the reaction of an alkali metal with molecular oxygen. For lithium-oxygen cells the discharge product was repeatedly identified as lithium peroxide.[26,27,37–40] In analogy to these findings, sodium peroxide formation was assumed in sodium-oxygen cells. In contrast to this assumption and the findings of some other research groups[29–32,41] we only found sodium superoxide (or hyperoxide).[33,34] To understand this phenomenon we took a closer look at the thermodynamic data of metal-oxygen cells. According to the equilibrium phase diagram the sodium-oxygen system (assuming bulk materials and excluding nanoscale effects) offers three feasible discharge products, of which of course only one is thermodynamically stable at fixed thermodynamics conditions.[42] In **Figure 1**a) the thermodynamic potential landscape is depicted. Three oxidation states of oxygen are possible: –0.5 for sodium superoxide (NaO_2), –1 for sodium peroxide (Na_2O_2) and –2 for sodium oxide (Na_2O). All thermodynamic data were taken from the database included in the software HSC Chemistry[10] and calculated on the reaction of two mole sodium with two mole oxygen (O_2) at standard conditions (T = 298 K and $p = 10^5$ Pa). In doing so, the free enthalpies of reaction can be directly compared.

The largest driving force is found for the reaction of sodium with oxygen to form sodium peroxide with a standard Gibbs reaction energy of $\Delta_r G° = -449.7$ kJ mol$(Na_2O_2)^{-1}$. Just slightly smaller is the driving force for the reaction to form sodium superoxide with $\Delta_r G° = -437.5$ kJ mol$(2\ NaO_2)^{-1}$. According to these data the Gibbs energy difference for the reaction

$$2NaO_2 \rightarrow Na_2O_2 + O_2 \quad (1)$$

is just –12.2 kJ mol$(Na_2O_2)^{-1}$. Considering that the thermodynamic data of less common compounds such as NaO_2 are always subject to some inaccuracy, it is also possible that sodium superoxide is the stable phase at standard conditions.[43] However, there is some evidence that the superoxide is indeed the less stable phase, as NaO_2 can only be prepared from Na_2O_2 by using extreme chemical conditions.[44]

The electric potential difference E of the galvanic cell depends on the reaction product and can be derived for the general reaction ($m = 1 \rightarrow NaO_2$; $m = 0.5 \rightarrow Na_2O_2$; $m = 0.25 \rightarrow Na_2O$)

$$Na + mO_2 = NaO_{2m} \quad (2)$$

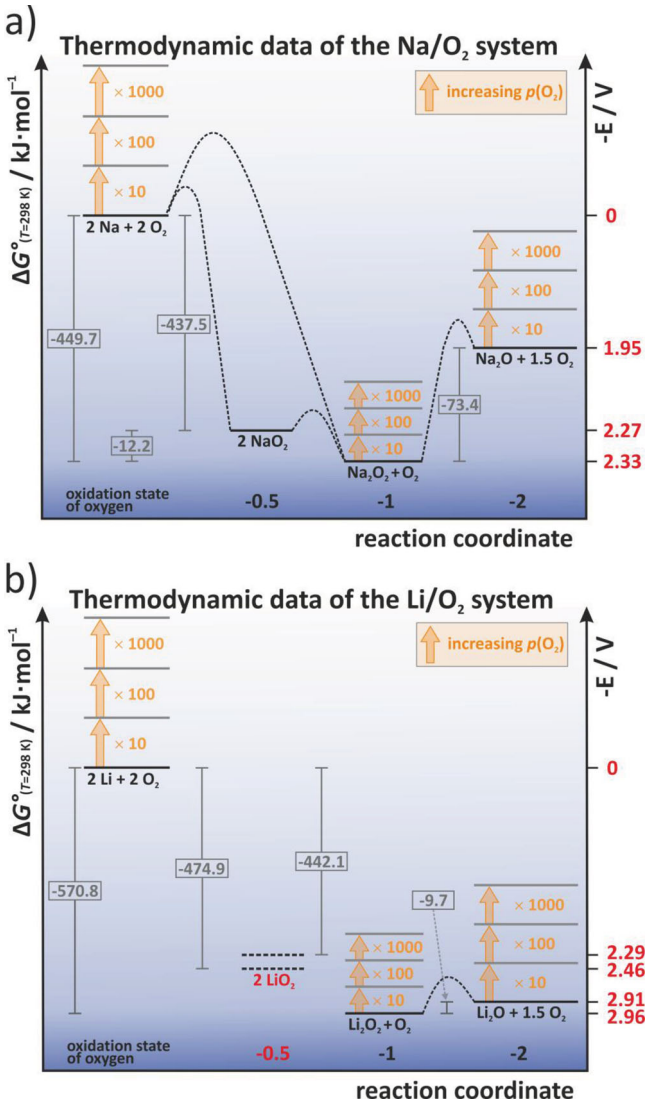

Figure 1. The thermodynamic landscape of a) sodium and b) lithium-oxygen cells. All values are calculated for the reaction $2A + 2O_2 \rightarrow A_2O_\gamma + (2 - \gamma/2)O_2$ (γ = 1,2,4). If not mentioned otherwise, thermodynamic data were taken from the database of HSC Chemistry Version 7.14.

$$\Delta_r G° = \mu°(NaO_{2m}) - \mu°(Na) - m\mu°(O_2) - RT \ln a^m(O_2) \quad (3)$$

$$E = -\frac{\Delta_r G}{F} = \frac{\mu°(NaO_{2m}) - \mu°(Na) - m\mu°(O_2)}{F} - \frac{mRT}{F} \ln a(O_2) \quad (4)$$

$$E = E° - \frac{mRT}{F} \ln\left(\frac{p(O_2)}{p(O_2) = 10^5\ \text{Pa}}\right) \quad (5)$$

The calculated standard cell potential differences $E°$ (at T = 298 K, $p(O_2) = 10^5$ Pa) from the thermodynamic data for sodium peroxide, superoxide and oxide are 2.33 V, 2.27 V and 1.95 V respectively. The values for the superoxide and the peroxide are very close, as expected, indicating that it is well possible to form either the superoxide or the peroxide in electrochemical cells.

As there is no data available on the activation energies it is not possible to discuss kinetic effects. But it is safe to assume that an one-electron transfer reaction is kinetically preferred compared to a two-electron transfer reaction, which favors sodium superoxide kinetically as final discharge product.

Oxygen is gaseous in its standard state, so $\Delta_r G°$ of the cell reaction and the relative stabilities of the different sodium oxide phases depend on the oxygen activity, i.e. the oxygen partial pressure as shown in Equation (5) ($a(\mathrm{Na}) = a(\mathrm{NaO}_x) = 1$). Increasing the oxygen partial pressure by one decade affects the relative stability in different ways. While the free enthalpy of the starting materials ($2\mathrm{Na} + 2\mathrm{O}_2$) rises by $2 \times 2.3RT \log(p(\mathrm{O}_2))$, i.e., by about 2×5.7 kJ mol^{-1} per decade of $p(\mathrm{O}_2)$, the corresponding data for the peroxide and oxide products only rise by $2.3RT \log(p(\mathrm{O}_2))$ = 5.7 kJ mol^{-1} and $1.5 \times 2.3RT \log(p(\mathrm{O}_2)) = 1.5 \times 5.7$ kJ mol^{-1} per decade of $p(\mathrm{O}_2)$, respectively. We note that for the given reactions in Figure 1 the superoxide level is not affected by the pressure change. A diagram on the phase stability as a function of oxygen partial pressure is also provided by Kang et al., however, based on first-principle calculations.[35] Hence, $-\Delta_r G$ for the superoxide formation reaction increases most strongly with increasing $p(\mathrm{O}_2)$ and is the most stable discharge product at elevated oxygen partial pressure. The red arrows and factors indicate the corresponding increases in oxygen activity. This is well in line with reported experimental conditions for the preparation of phase pure sodium superoxide in which sodium peroxide reacts with oxygen at partial pressures and temperatures of approximately 280×10^5 Pa and 475 °C.[44] Taking the calculated value −12.2 kJ mol$(\mathrm{Na_2O_2})^{-1}$ (see Equation (1)) for the standard free enthalpy of reaction from the superoxide to the peroxide, we estimate an oxygen pressure of 133×10^5 Pa as minimum value to shift the equilibrium to $\mathrm{NaO_2}$, which is in reasonable agreement with the experiment in view of the uncertainty in the thermodynamic data of $\mathrm{NaO_2}$. As mentioned in the introduction, theoretical calculations by Lee et al. indicate that bulk $\mathrm{NaO_2}$ is indeed thermodynamically more stable than bulk $\mathrm{Na_2O_2}$ at standard conditions, while Kang et al. report that a minimum $p(\mathrm{O}_2)$ of 8.5 atm is required.[35] Kang et al. also report that $\mathrm{NaO_2}$ will be thermodynamically (at standard conditions) only more stable than $\mathrm{Na_2O_2}$ below a particle size of about 10 nm.[36]

The situation for the Li-O system is shown in Figure 1b. At first glance the data look quite similar, but in contrast to the Na-O system there are only vague data on the lithium superoxide known. Contrary to $\mathrm{NaO_2}$ (and other alkali superoxides), lithium superoxide could yet not be isolated as a solid phase. In the calculated Li-O phase diagram the $\mathrm{LiO_2}$ phase does not exist, and we can assume it to be unstable.[45] The current data for $\mathrm{LiO_2}$ are taken from reference[46,47] where the authors estimated values for $\Delta_r G°$. Compared to the Na-O system, the driving forces for the reactions in Figure 1b) are a bit larger with $\Delta_r G° = -570.8$ kJ mol$(\mathrm{Li_2O_2})^{-1}$ for $\mathrm{Li_2O_2}$, $\Delta_r G° = -561.2$ kJ mol (2 $\mathrm{Li_2O})^{-1}$ for $\mathrm{Li_2O}$ and $\Delta_r G° \approx -460$ kJ mol$(\mathrm{Li_2O})^{-1}$ for $\mathrm{LiO_2}$. Interestingly the difference between $\mathrm{Li_2O_2}$ and $\mathrm{Li_2O}$ in the reaction

$$\mathrm{Li_2O_2} \rightarrow \mathrm{Li_2O} + 0.5\mathrm{O_2} \quad (6)$$

is only 9.7 kJ mol$(\mathrm{Li_2O_2})^{-1}$, so that $\mathrm{Li_2O}$ has to be considered as possible (side) discharge product, just as $\mathrm{NaO_2}$ in the case of sodium, but at low oxygen activities. But the further oxidation of oxygen to form the oxide from the peroxide requires the oxygen–oxygen bond to break, which is kinetically not favored. Correspondingly the potentials of the different discharge products are very similar with 2.96 V for $\mathrm{Li_2O_2}$ and 2.91 V for $\mathrm{Li_2O}$. The expected free enthalpy of the superoxide is about 100 kJ mol^{-1} higher, which clearly favors the reaction to the peroxide. Obviously the driving force for peroxide formation is much stronger for lithium than for sodium. The thermodynamics of the Li-O system explains why $\mathrm{LiO_2}$ has only been found as intermediate species in lithium-oxygen cells and why the synthesis of phase pure $\mathrm{LiO_2}$ has not been successful yet. Assuming that the thermodynamic data for $\mathrm{LiO_2}$ is more or less accurate, its synthesis should be theoretically possible only at extremely high oxygen partial pressures ($p(\mathrm{O}_2) > 10^{22}$ Pa).

Besides discussing the net cell reaction between sodium and oxygen it is also worth considering possible side reactions that might be quite similar to reactions known from lithium-oxygen cells, e.g., reactions with the carbon positive electrode or water in the electrolyte or the gas phase. In Figure S1 (Supporting Information) we have sketched the corresponding thermodynamic landscapes for sodium and lithium. Considering the reaction of sodium with oxygen and carbon there is a large driving force to form sodium carbonate ($\Delta_r G° = -1047$ kJ mol^{-1}). Also the reaction of the discharge products $\mathrm{NaO_2}$, $\mathrm{Na_2O_2}$ and $\mathrm{Na_2O}$ with carbon is favored with a $\Delta_r G°$ of about −600 kJ mol^{-1} referring to one mol of $\mathrm{Na_2CO_3}$. Keeping in mind that almost every positive electrode in metal-oxygen cells contains carbon as conductive additive and structural support, carbonate formation will probably be an unavoidable side reaction. Other exergonic reactions are possible including decomposition of the electrolyte, binder and other cell parts. Besides, also $\Delta_r G°$ for the reaction of water with several cell components is negative too (see Supporting Information Table S1). Water can either react to form sodium hydroxide or it can react with sodium peroxide to form the dihydrate or the octahydrate.[30,48]

Even though this simple thermodynamic treatment is straightforward it needs to be emphasized that the side reactions do not necessarily prevent the viable function of a metal-oxygen cell once kinetic effects suppress the side reactions. Lithium-ion batteries commonly operate outside the thermodynamically stability limit of some of the cell components, and their comparably long lifetime is, by and large, a result of minimizing and delaying side reactions by many different measures. However, thermodynamic screening for energetically favored side reactions is very useful in predicting the most severe degradation mechanisms that should be considered.

Summarizing the thermodynamic assessment it is obvious that both $\mathrm{NaO_2}$ and $\mathrm{Na_2O_2}$ are possible discharge products in sodium-oxygen cells, whereas $\mathrm{LiO_2}$ only appears as comparably unstable intermediate in lithium-oxygen cells. Furthermore, formation of $\mathrm{Na_2O}$ instead of $\mathrm{Na_2O_2}$ is much less favored compared to the formation of $\mathrm{Li_2O}$ instead of $\mathrm{Li_2O_2}$. Even though the driving forces for side reactions are smaller in the case of sodium, still many reactions between the discharge products (oxides, peroxides, superoxides) and impurities or cell components are thermodynamically quite favored.

We note that we do not report experimental results on the oxygen activity dependence of the cell reaction in the present

paper. In order to achieve well reproducible experimental conditions (e.g., avoiding loss of solvent or contamination by impurities in flowing gas) we worked with closed cells and a limited volume of gas. Therefore the proper and quantitative control of oxygen activity in the cell gas volume beyond the activity 1 of pure oxygen was not possible. The study of more complex reaction conditions in flowing gas atmosphere will be part of future experimental studies. As already stated, the discharge product appears to be kinetically controlled, and therefore, we addressed experimentally those factors that can have major impact on the reaction route, such as the type of carbon electrode.

2.2. Impact of the Type of Carbon

From the recent results reported on sodium-oxygen batteries, it appears that the type of carbon might have a major impact on the amount and type of discharge product. For instance Kim et al. used carbon black (Ketjenblack) and found sodium carbonate as the discharge product using carbonate based electrolytes (2800 mAh g^{-1}) and sodium peroxide using an ether based electrolyte (6000 mAh g^{-1}).[31] By using graphene nanosheets Liu et al. found sodium peroxide to be the discharge product (9268 mAh g^{-1}).[29] Finally Sun et al. detected sodium peroxide and sodium carbonate in their cells while using diamond-like carbon (3600 mAh g^{-1}).[30] Nevertheless the results so far do not show a clear correlation between surface structure/chemistry and product control or achievable capacity.

In order to study whether the type of carbon has any impact on the cell reaction at all, we carried out a systematic study of several carbon materials with different properties and compared them with our reference positive electrode that we employed in all earlier studies, namely a gas diffusion layer (GDL) H2315 (<1 m^2 g^{-1}) from Freudenberg & Co. KG. The other carbons being tested were Ketjenblack EC 600 JD (1454 m^2 g^{-1}), Super PLi (62 m^2 g^{-1}), HSAG 500 (490 m^2 g^{-1}), SFG-44 (5.5 m^2 g^{-1}) and the templated carbon SCR-1 (565 m^2 g^{-1}). These carbons cover a wide range of properties such as high and low surface areas, different particle sizes and shapes and surface chemistry. More detailed information on the carbon materials can be found in Table S2 (Supporting Information). All carbons, except the GDL that is free standing, were spray coated on a glass fiber separator as support. The cathodes were tested in otherwise identical cells with 3 electrode arrangement and the discharge products were studied by X-ray diffraction and scanning electron microscopy. We note that from our experience, knowledge of the exact cell design might be a very critical parameter when reproducing experimental data from other groups. We therefore provide detailed information on our in-house developed cell design (Giessen cell) in the Supporting Information.

In **Figure 2**a the resulting discharge and charge hysteresis of the first cycle are shown. Panel (a) shows the absolute capacity whereas (b) shows the capacity normalized to the mass of carbon.

For the absolute capacity the GDL shows the best performance with about 2.3 mAh followed by the HSAG carbon with 2.0 mAh, Super PLi with 1.4 mAh, Ketjenblack with 1.2 mAh, SFG-44 with 0.7 mAh and SCR-1 with 0.4 mAh. All measurements were run at a current density of 200 µA cm^{-2} (geometrical area of the electrode) and within a potential window between 1.8 V and 2.6 V. We limited the potential to 2.6 V to suppress side reactions occurring at higher potentials (Figure S5, Supporting Information). The ranking changes

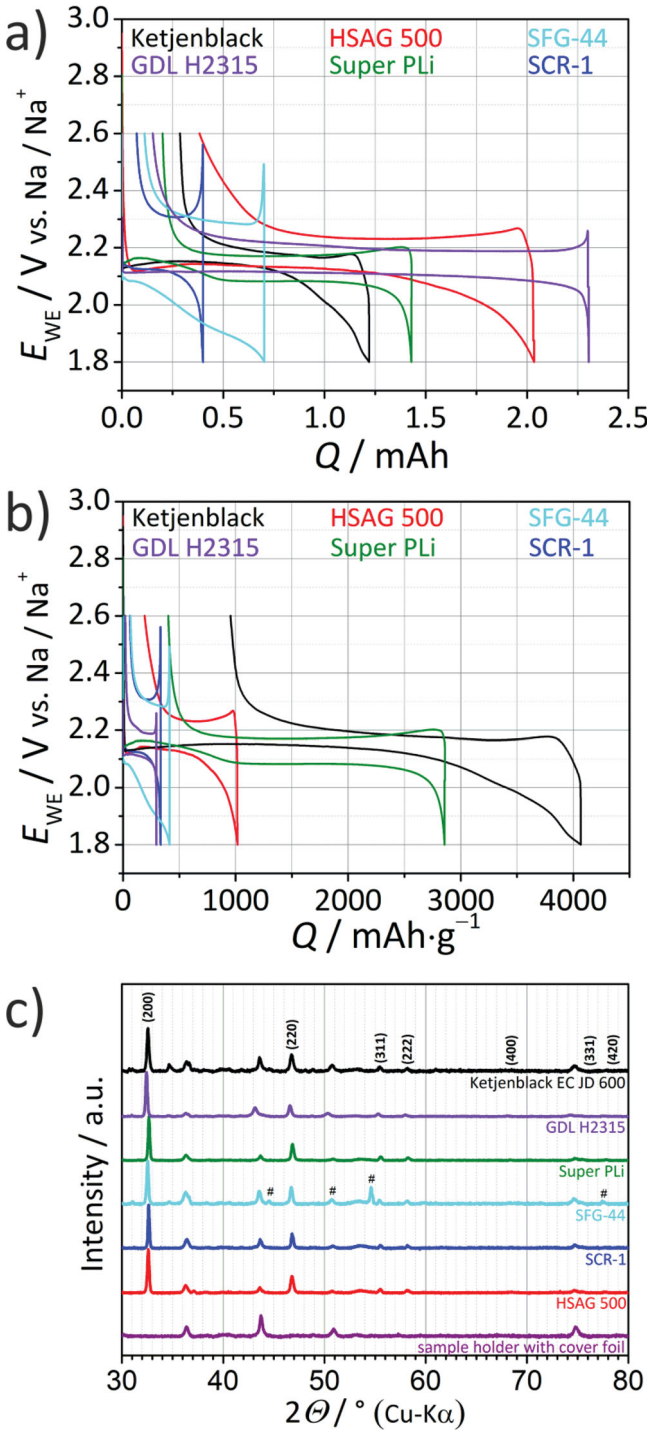

Figure 2. a) Discharge and charge potential hysteresis for sodium-oxygen-cells with different carbon cathodes (200 µA cm^{-2}). b) The same plot just with the reference to the carbon mass in the electrode. c) X-ray diffraction pattern of discharged cells with different carbons used in the cathode. # denotes diffraction lines of graphite.

Table 1. Average discharge capacities of the six tested carbon materials in sodium-oxygen cells. All cells were cycled at a geometrical current density of $j = 200$ μA cm^{-2}. Depending on the normalization different carbons are revealed as the best choice. The geometrical area of all cathodes (10 mm in diameter) was 0.785 cm^2.

Carbon	Q_{dis} [mAh]	Efficiency 1st cycle [%]	m [mg]	Q_{dis} [mA h g^{-1}]	S_{BET} [m^2 g^{-1}]	Q_{dis} [mAh m^{-2}]	j_{local} [μA cm^{-2}]
H2315	2.3	93.5	7.8	295	1.0	294.87	2.00
SFG-44	0.7	84.3	1.5	467	5.5	84.85	1.89
Super PLi	1.4	85.7	0.5	2800	62.0	45.16	0.50
Ketjenblack EC 600JD	1.2	75.8	0.3	4000	1454	2.75	0.04
HSAG 500	2.0	81.0	2.0	1000	490	2.04	0.02
SCR-1	0.4	82.5	1.2	333	565	0.59	0.02

completely by comparing the discharge capacity with respect to the amount of carbon on the electrode. Due to its large mass of 7.8 mg the GDL now shows the smallest discharge capacity of 295 mAh g^{-1}_{carbon}. The electrode made of Ketjenblack is, due to its very low carbon loading of only 0.3 mg, noticeably better and reaches a discharge capacity of 4000 mAh g^{-1}_{carbon}. All of the other carbons spread in between these two values depending on their loading on the electrode. We note that the GDL is a free standing electrode whereas the other electrodes consist of carbon sprayed onto a glass fiber separator as support. As it is common in the literature, we did not include the weight (≈4.4 mg) of this separator support and normalized to the mass of carbon only. Taking into account that the product deposits on the surface of the carbon, in the next step we normalized to the effective surface area of the carbon. Doing so, the ranking of the most effective carbon cathode material is shuffled again (Figure S2, Supporting Information). These simple differences in normalization illustrate the difficulties when trying to compare capacity values in the field of metal-oxygen cells. Needless to say that a direct comparison between different values reported in literature is only possible if and when all essential experimental details (achieved capacities, cell dimensions, amount of carbon, etc.) are provided; these facts are often provided only incompletely in literature making reported capacity values hardly comparable to other publications. From the present study, the GDL appears most suitable to study the cell chemistry of sodium-oxygen cells as the maximum absolute capacity is achieved which eases the characterization of the discharge product and also improves the signal when following pressure changes during galvanostatic cycling.[49] However, when developing a practical device the choice might be of course different. **Table 1** summarizes the absolute discharge capacities achieved for the different carbon materials and normalized with respect to the weight and BET surface area of the carbon materials. We also included the current density based on the total surface area of the different carbon electrodes in this table.

A closer look at the discharge and charge hysteresis reveals similarities and differences in cell potentials between the different kinds of carbons. During discharge one plateau can be observed for all carbons at around 2.15 V vs. Na/Na$^+$. The end of discharge is characterized by a sharp potential drop (sudden death) to 1.8 V for the GDL, SCR-1 and Super PLi. In case of HSAG-500, Ketjenblack and SFG-44 the cut off at 1.8 V vs. Na/Na$^+$ is reached by a sloped decrease in potential. The Coulomb efficiency (Q_{chg}/Q_{dis}) for every type of carbon is around 90% with the H2315 and Ketjenblack 600JD showing the highest and lowest values.

During charge the cells behaviors differ again. Cells with SFG-44, SCR-1 and GDL show a peak at the beginning of the charging process while cells with Ketjenblack, Super PLi and HSAG 500 do not. Generally, an initial peak during charging is associated with an activation barrier. Even though we cannot finally conclude on this, it can be seen that the intensity depends on the specific surface area of the carbon materials, i.e., the lower the surface, the more pronounced is the peak.

In any case, as a result of using structurally very different carbon materials we observed appreciable differences in the maximum capacity and voltage profiles. However, these differences cannot be traced back to chemically different products, i.e., a change from NaO_2 to Na_2O_2. To determine the nature of the discharge product we performed X-ray diffraction measurements of the carbon cathodes after discharge (Figure 2c). All carbon electrodes showed a similar diffraction pattern. For a better comparison the data have been normalized to the most intense reflex, which was in all cases the (200) reflex of NaO_2 referring to the pdf card 01-077-0207. The comparison of the different diffraction patterns clearly proves that the discharge product is always NaO_2, independent of the used carbon material. We do not find any evidence for another discharge product besides NaO_2 when using different carbon materials as positive electrodem with our cell setup and gas supply. The small diffraction line at 31° can be assigned to the conducting salt sodium triflate (Figure S3, Supporting Information) and the diffraction line at 34.7° may belong to sodium sulfite Na_2SO_3 (pdf 01-070-1909) for that we earlier found evidence by X-ray photoelectron spectroscopy (XPS).[34] Clearly, other parameters than the type of carbon material must be responsible for the formation of other discharge species in sodium-oxygen cells.[28,29,31,34,50] Thus, future research efforts should also include quantification of discharge products in relation to the achieved discharge capacities[34,51] and studies on the influence of the electrolyte composition (and possible impurities) on the product formation. However, from our experience gained so far we have no indication for a significant impact of the latter on the discharge product in a variety of ether based electrolytes either (Figure S3, Supporting Information).

2.3. Cycle Life

Improving cycle life is currently one of the major tasks in metal-oxygen battery research. For example, until recently there was hardly any experimental evidence for a reversible formation of Li_2O_2 over prolonged cycling.[39,52,53] Although we could prove reversible formation of sodium superoxide in our cells for several cycles, the total capacity faded quickly, and only negligible capacities were obtained after ten cycles.[34] Liu et al. reported also short cycle life with a maximum of 10 cycles in ether based sodium-oxygen cells.[29]

We found that the decomposition of the conductive salt (NaOTf) might be one of the key issues preventing long cycle life, but have yet not succeeded in finding better suited salts. Therefore, we use shallow cycling as an approach to increase cycle life which is frequently applied in lithium-oxygen cells.[39,53] Shallow cycling is a well-known procedure to improve the cycle life of batteries in general which also considerably improves the results for lithium-oxygen cells. The standard cell discharge/charge experiment is normally done galvanostatically until fixed cut-off potentials are reached. Given the defined voltage plateaus during cell discharge of lithium- and sodium-oxygen cells, applying cut-off potentials corresponds to deep cycling (100% depth of discharge). In a capacity limited mode (shallow cycling), galvanostatic discharging and charging is restricted by defining the amount of charge that is electrochemically converted (cut-off capacity). For the latter, the depth of discharge can be considerably smaller than 100%. Following this concept we investigated the difference between deep cycling (here cut-off potentials of 1.8 V to 2.6 V were applied) and shallow cycling. Cut-off capacities of 0.5 mAh were chosen, but the measurements also stopped in case that the cell potential exceeds the cut-off potentials defined in the deep cycling protocol. For this study, we restricted the experiments to those carbon materials that showed the highest capacity values, i.e., the GDL and Ketjenblack. **Figure 3** shows the difference between deep cycling and shallow cycling for two equivalent sodium-oxygen-cells with a GDL cathode.

The discharge and the charging potential plateaus of both cells are very similar with about 2.1 V vs. Na^+/Na and about 2.2 V vs. Na^+/Na, respectively. At ≈80% of charge the potential increases exponentially and the cell runs into the cut-off voltage of 2.6 V vs. Na^+/Na. This is a very important feature of the sodium superoxide cell showing that the charging ends as soon as almost the entire discharge product has vanished. The cut-off potential of 2.6 V vs. Na^+/Na was set in order to minimize any possible electrolyte decomposition reactions (Figure S5, Supporting Information). The most notable difference can be

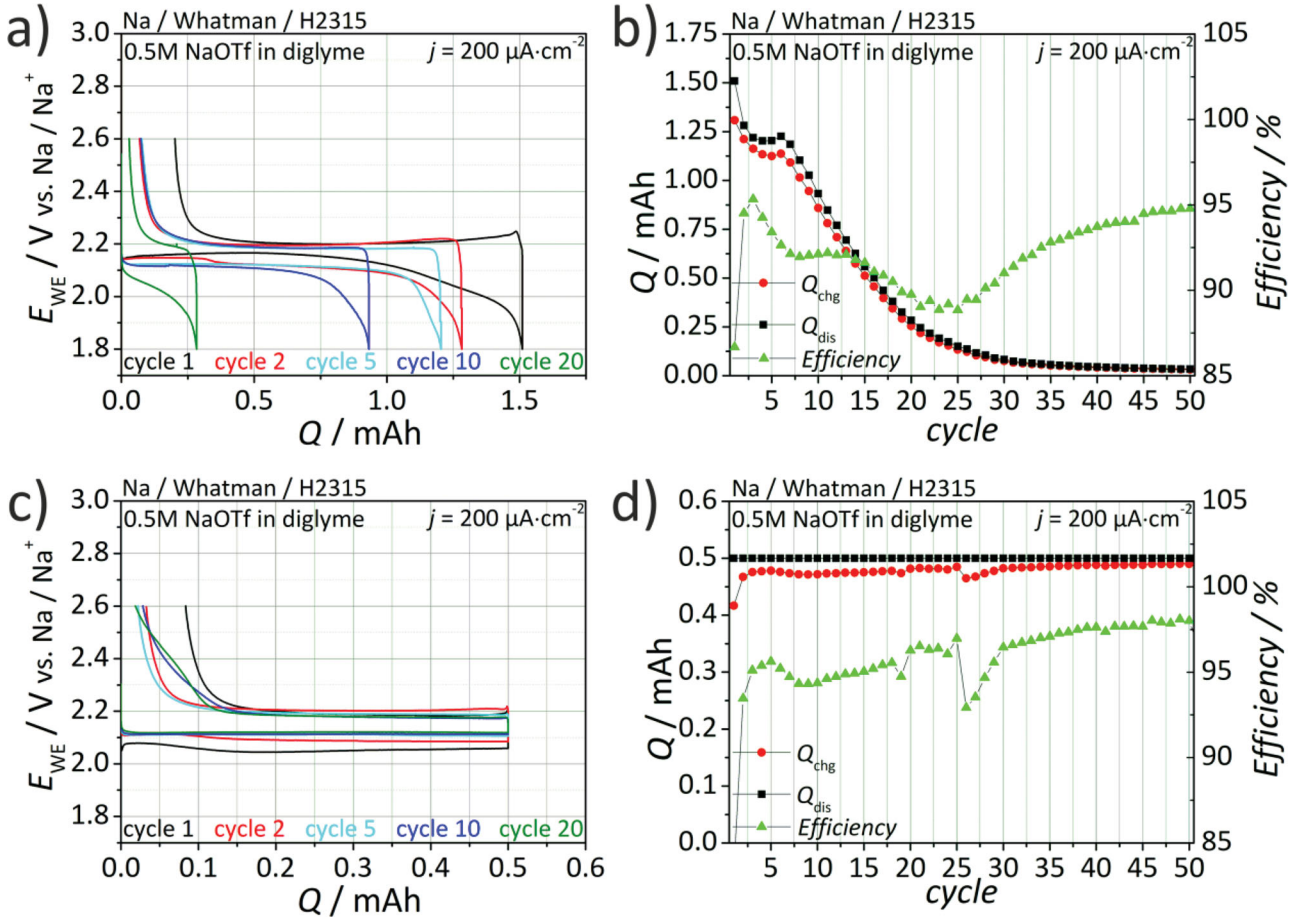

Figure 3. Comparison of two analogous sodium-oxygen cells: a,b) Deep cycling (100% DOD) between 1.8 V and 2.6 V and c,d) shallow cycling with a capacity cut off at 0.5 mAh, which is around 33% of full discharge capacity.

seen when comparing the cycle life of the two cells. While deep cycling leads to a rapid capacity fading, shallow cycling enables a steady performance. Also, only a negligible change in the cell potentials is observed. The overpotential during discharge actually slightly decreases upon cycling. For the deep cycled cell, the overpotential increases upon cycling. Of course, a critical question is whether also more charge was converted in the shallow cycled cell. Within the first 50 cycles the amount of charge converted in the deep cycled cell shows a summed up discharge capacity of 19.8 mAh while the shallow cycled cell shows 25 mAh. On charge the values are 18.2 mAh (92.0% efficiency) and 24.0 mAh (96.0% efficiency). Thus, from the point of view of cycle life shallow cycling is superior to deep cycling. Presumably side reactions occurring at potentials below 2.0 V are responsible for the poor cycle life when cells are deep discharged. However, with respect to the aim of a high capacity per cycle shallow cycling is critical.

Figure 4 shows the results for the Ketjenblack electrode. At first glance there is no obvious difference to the GDL. But following the comparability issue for achievable discharge capacities one has to be careful again: Even though the absolute capacity (in mAh) is exactly the same, the cell with Ketjenblack shows a way higher specific capacity, 1666 mAh g^{-1} vs. 64 mAh g^{-1}, when normalizing to the mass of carbon. On the other hand comparing the capacity per carbon surface area it is only 1.2 mAh m^{-2} for Ketjenblack and 64.0 mAh m^{-2} for the gas diffusion layer GDL. Of course, normalized to the geometrical electrode area, the capacity is identical again. Panel c) and d) of Figure 4 show the GDL and the Ketjenblack electrode after discharge to 1.5 mAh. Both electrodes are fully covered with cubes in the typical shape of sodium-superoxide crystals.[33,34] Although the shape is the same, the crystals differ in size and number. For the GDL few large individual particles cover the fibers while the surface of the Ketjenblack is fully covered with many, but smaller particles. The biggest particles are 18 µm in edge length for GDL and 8 µm for Ketjenblack. It appears that the GDL has less nucleation sites than Ketjenblack which corresponds to the surface area and the particle size of both carbons.

2.4. Comment on the Shallow Cycling Procedure

Obviously the shallow cycling procedure considerably improves the cycle life. However, a balanced view on the advantages and disadvantages of this procedure is necessary. The penalty that

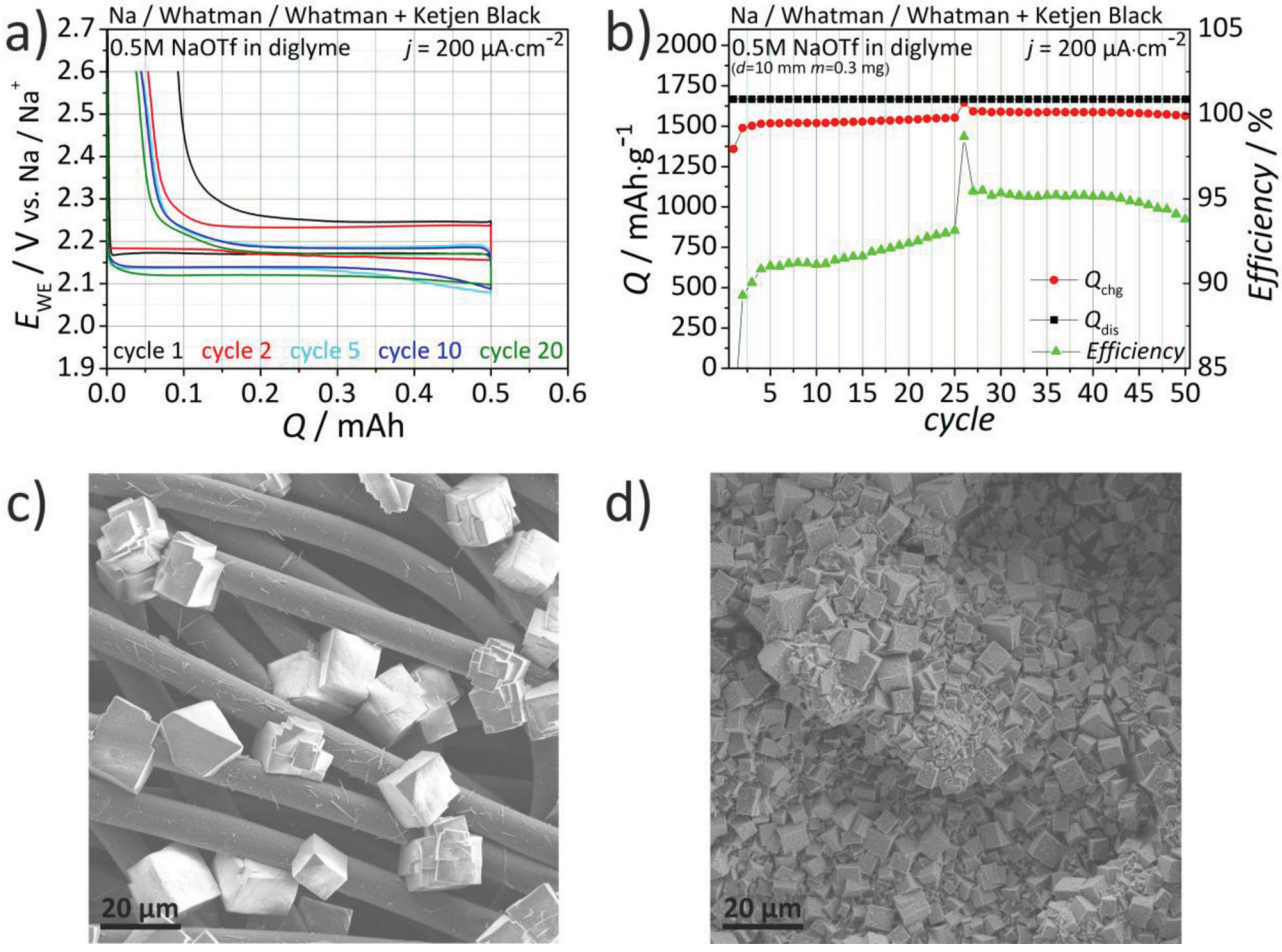

Figure 4. a) Voltage profiles and b) cyclability of a shallow cycled cell with Ketjenblack and associated SEM images of discharged cathodes of c) GDL and d) Ketjenblack.

has to be paid for the improvement in cycle life is a decrease in cell capacity and hence energy density. For our current experiments, the capacity cut-off was set to 0.5 mAh (or 1600 mAh g^{-1}) that corresponds to about one third of the capacity that is achieved by deep cycling, i.e., 33% DOD.

To get a better view of shallow cycling it is useful to consider commercial lithium ion batteries (LIBs) and their electrode performance. Lithium cobalt oxide (Li_xCoO_2, LCO) is still widely used as active material for the positive electrode. Taking a typical 18650 cell from Sony as example, Ramadass et al. showed that practical specific capacity values are around 145 mAh $g(LCO)^{-1}$.[54] Such capacity values are easily reached for Li-O_2 positive electrodes. However the electrode area in a practical cell is limited and it is necessary to achieve a certain area capacity as well. The LCO area loading in the cell investigated by Ramadass et al. was 28.4 mg cm^{-2}[54] corresponding to an area capacity of approx. 4.1 mAh cm^{-2}. This means that building a Li-O_2 cell with an energy density comparable to a commercial LIB requires more than 5 mAh cm^{-2} for the positive electrode, taking into account the higher cell voltage of the LIB. Thus a Li-O_2 positive electrode delivering lower area capacities, e.g., as a result of shallow cycling, can easily lose its expected advantages. Of course, research on Li-O_2 cells is still on a relatively fundamental level and practical cell energy densities depend on many factors. But it appears certainly useful that in addition to gravimetric capacities also area capacities should be stated. For the present Na/O_2 cell and using a GDL cathode, we so far achieved values of 2.93 mAh cm^{-2} for deep cycling, and 0.64 mAh cm^{-2} for the shallow cycling procedure, which are reasonable values considering the early research state. However, it also shows that future efforts also need to be directed towards further increasing the area capacity.

3. Conclusion

The Na/O_2 battery and the comparison of its performance with the much longer studied Li/O_2 battery currently give rise to several intriguing questions: Why is Li_2O_2 found as sole discharge product in Li/O_2 cells, whereas both NaO_2 and Na_2O_2 have been reported for Na/O_2 cells? Is it possible to deliberately steer the cell reaction to form NaO_2 or Na_2O_2 or a mixture of both? How and for how long can the cycle life of Na/O_2 cells be improved? Can meaningful absolute capacities be achieved? While it is still a long way to finally answer all these questions in detail we can conclude from our present study the following. Firstly, the thermodynamic assessment revealed that NaO_2 formation might well compete with Na_2O_2 formation whereas Na_2O formation is thermodynamically unfavorable. This explains why both NaO_2 and Na_2O_2 have been reported as discharge product in sodium-oxygen cells and only slight variations in cell design or cycling conditions could benefit the formation of one or the other compounds (or mixtures of them). Secondly, the impact of the type of carbon on the nature of the discharge product and the achievable capacities was studied. We found that for the studied cell design, the product is always NaO_2 even though a broad range of structurally very different carbon materials has been employed. Therefore other, maybe more hidden parameters, are more likely to be responsible for the different findings reported in literature. On the other hand, the achievable discharge capacities strongly depend on the type of carbon and values ranging from 300 mAh g^{-1} and 4000 mAh g^{-1} can be obtained. However, we also discussed that capacity values normalized on the amount of carbon can be quite misleading. Thirdly, we showed that shallow cycling can be used to considerably improve the cycle life of sodium-oxygen batteries with stable capacity values of around 64 mAh g^{-1} for at least 80 cycles using a GDL and 1666 mAh g^{-1} for at least 60 cycles using Ketjenblack. The penalty for shallow cycling is a decrease in energy density which has to be critically evaluated when considering metal/oxygen batteries for high energy density applications. A careful balance between achieving long life time and sacrificing energy density is therefore necessary.

4. Experimental Section

Cathode Preparation: For the experiments two kinds of positive electrodes were used. A binder-free gas diffusion layer (Freudenberg H2315, Quintech) was used and for comparison different kinds of carbons on a glass microfiber filter (GF/A, Whatman) were prepared. To do so 300 mg carbon was mixed with 50 mg PTFE solution (60 wt% PTFE dispersion in water, Sigma-Aldrich) and 30 mL Acetone (CHROMASOLV >99.9%, Sigma-Aldrich) and stirred the solution for 10 min with a dispermix (X10, Ystral) at highest level. Then this slurry was directly sprayed on a glass microfiber filter (GF/A, Whatman). After drying, electrodes with a diameter of 10 mm were punched and dried in vacuum at 140 °C for 24 h. The average carbon loading depends on the kind of carbon and ranged from 0.2 mg up to 4.0 mg. The electrode area was 0.785 cm^2. No catalyst was used in any case.

Cell Assembly: Electrochemical tests were performed using the Giessen cell, a cell based on a modified Swagelok design, which is described in the supporting information. The negative electrode consisted of pure sodium metal (donated by BASF SE) with a diameter of 12 mm while the positive electrode was 10 mm in diameter. Two glass microfiber filter (GF/A, Whatman, Ø 12 mm) were used to separate the electrodes. Diglyme (anhydrous, 99.5% Sigma Aldrich) was used as the solvent and sodium triflate ($NaSO_3CF_3$, 98%, Aldrich) was used as conducting salt for the electrolyte. Diglyme was dried over molecular sieves (3 Å for 1 week), sodium triflate under vacuum at 110 °C for 24 h. The final water content of the electrolyte was determined with an 831KF Karl Fischer coulometer (Metrohm) to be less than 15 ppm. Every cell contained 70 µL of electrolyte with additional 10 µL for connection of the reference electrode. Preparation and handling of the electrolyte as well as cell assembly were carried out in an argon-filled-glove-box (GST4, Glovebox Systemtechnik) with water and oxygen contents below 5 ppm.

Electrochemical Cell Testing: All cells were cycled galvanostatically (constant current) in a climate chamber at 25 °C using a battery cycling system 4300 from Maccor. The cell design consists of an oxygen reservoir of about 9 cm^3, which was flushed with oxygen (purity 5.0, Praxair) for 10 s at 10^5 Pa just before the measurement. The cut-off limits were set to 1.8 V vs. Na^+/Na and 2.6 V vs. Na^+/Na respectively. For shallow cycling a capacity limit of 0.5 mAh was set.

Structural Characterization: Discharged positive electrodes were analyzed using an X'Pert Pro (PANalytical) powder X-ray diffractometer (Cu-K source, 40 kV, 40 mA). A self-made gas-tight sample holder was used for these structural characterizations. The specific surface area (Brunauer-Emmett-Teller) was determined by nitrogen physisorption at 77 K using an Autosorb-1 machine from Quantachrome Instruments. Elementary analysis was performed on a Vario MICRO Cube CHNSO (ELEMENTAR Analysensysteme). SEM measurements were performed on a Merlin high-resolution Schottky field-emission electron microscope (Zeiss SMT) equipped with an X-Max EDS detector (Oxford Instruments).

Supporting Information

Supporting Information is available from the Wiley Online Library or from the author.

Acknowledgement

C.L.B. thanks Fonds der Chemischen Industrie for a Ph.D. scholarship. The project was supported by the BASF International Scientific Network for Electrochemistry and Batteries. The authors thank Christine Raiss for nitrogen physisorption measurements, CHNSO analysis and for providing the SCR-1 carbon.

Received: December 5, 2013
Revised: March 17, 2014
Published online:

[1] J. Christensen, P. Albertus, R. S. Sanchez-Carrera, T. Lohmann, B. Kozinsky, R. Liedtke, J. Ahmed, A. Kojic, *J. Electrochem. Soc.* **2012**, *159*, R1.
[2] J. Yang, D. Zhai, H.-H. Wang, K. C. Lau, J. a. Schlueter, P. Du, D. J. Myers, Y.-K. Sun, L. a Curtiss, K. Amine, *Phys. Chem. Chem. Phys.* **2013**, *15*, 3764.
[3] B. M. Gallant, D. G. Kwabi, R. R. Mitchell, J. Zhou, C. V. Thompson, Y. Shao-Horn, *Energy Environ. Sci.* **2013**, *6*, 2518.
[4] Z. Peng, S. a. Freunberger, L. J. Hardwick, Y. Chen, V. Giordani, F. Bardé, P. Novák, D. Graham, J.-M. Tarascon, P. G. Bruce, *Angew. Chem. Int. Ed.* **2011**, *50*, 6351.
[5] T. Zhang, N. Imanishi, S. Hasegawa, A. Hirano, J. Xie, Y. Takeda, O. Yamamoto, N. Sammes, *Electrochem. Solid-State Lett.* **2009**, *12*, A132.
[6] H. He, W. Niu, N. M. Asl, J. Salim, R. Chen, Y. Kim, *Electrochim. Acta* **2012**, *67*, 87.
[7] Y. Wang, H. Zhou, *J. Power Sources* **2010**, *195*, 358.
[8] K. W. Semkow, A. F. Sammeils, *J. Electrochem. Soc.* **1987**, *134*, 2084.
[9] K. M. Abraham, Z. Jiang, *J. Electrochem. Soc.* **1996**, *143*, 1.
[10] Outotec Research Center, *HSC Chem. 7.14 database*.
[11] J. Janek, P. Adelhelm, in *Handb. Lithium-Ionen-Batterien,* (Ed: R. Korthauer), Springer-Verlag, Berlin Heidelberg **2013**.
[12] B. D. McCloskey, A. Speidel, R. Scheffler, D. C. Miller, V. Viswanathan, J. S. Hummelshøj, J. K. Nørskov, A. C. Luntz, *J. Phys. Chem. Lett.* **2012**, *3*, 997.
[13] D. Sharon, V. Etacheri, A. Garsuch, M. Afri, A. A. Frimer, D. Aurbach, *J. Phys. Chem. Lett.* **2013**, *4*, 127.
[14] V. S. Bryantsev, J. Uddin, V. Giordani, W. Walker, D. Addison, G. V. Chase, *J. Electrochem. Soc.* **2012**, *160*, A160.
[15] W. Walker, V. Giordani, J. Uddin, V. S. Bryantsev, G. V Chase, D. Addison, *J. Am. Chem. Soc.* **2013**, 3.
[16] W. Xu, J. Hu, M. H. Engelhard, S. a. Towne, J. S. Hardy, J. Xiao, J. Feng, M. Y. Hu, J. Zhang, F. Ding, M. E. Gross, J.-G. Zhang, *J. Power Sources* **2012**, *215*, 240.
[17] B. D. McCloskey, D. S. Bethune, R. M. Shelby, G. Girishkumar, A. C. Luntz, *J. Phys. Chem. Lett.* **2011**, *2*, 1161.
[18] S. A. Freunberger, Y. Chen, N. E. Drewett, L. J. Hardwick, F. Bardé, P. G. Bruce, *Angew. Chem. Int. Ed.* **2011**, *50*, 8609.
[19] Z. Zhang, J. Lu, R. S. Assary, P. Du, H.-H. Wang, Y.-K. Sun, Y. Qin, K. C. Lau, J. Greeley, P. C. Redfern, H. Iddir, L. a. Curtiss, K. Amine, *J. Phys. Chem. C* **2011**, *115*, 25535.
[20] Y. Chen, S. A. Freunberger, Z. Peng, F. Bardé, P. G. Bruce, *J. Am. Chem. Soc.* **2012**, *134*, 7952.
[21] V. S. Bryantsev, F. Faglioni, *J. Phys. Chem. A* **2012**, *116*, 7128.
[22] V. S. Bryantsev, V. Giordani, W. Walker, M. Blanco, S. Zecevic, K. Sasaki, J. Uddin, D. Addison, G. V Chase, *J. Phys. Chem. A* **2011**, *115*, 12399.
[23] D. Xu, Z.-L. Wang, J.-J. Xu, L.-L. Zhang, L.-M. Wang, X.-B. Zhang, *Chem. Commun.* **2012**, 11674.
[24] K. U. Schwenke, S. Meini, X. Wu, H. a Gasteiger, M. Piana, *Phys. Chem. Chem. Phys.* **2013**, *15*, 11830.
[25] D. Sharon, V. Etacheri, A. Garsuch, M. Afri, A. a. Frimer, D. Aurbach, *J. Phys. Chem. Lett.* **2013**, *4*, 127.
[26] M. M. Ottakam Thotiyl, S. A. Freunberger, Z. Peng, Y. Chen, Z. Liu, P. G. Bruce, *Nat. Mater.* **2013**, *12*, 1050.
[27] M. M. Ottakam Thotiyl, S. A. Freunberger, Z. Peng, P. G. Bruce, *J. Am. Chem. Soc.* **2013**, *135*, 494.
[28] E. Peled, D. Golodnitsky, H. Mazor, M. Goor, S. Avshalomov, *J. Power Sources* **2011**, *196*, 6835.
[29] W. Liu, Q. Sun, Y. Yang, J.-Y. Xie, Z.-W. Fu, *Chem. Commun.* **2013**, 3.
[30] Q. Sun, Y. Yang, Z.-W. Fu, *Electrochem. Commun.* **2012**, *16*, 22.
[31] J. Kim, H.-D. Lim, H. Gwon, K. Kang, *Phys. Chem. Chem. Phys.* **2013**, *15*, 3623.
[32] S. K. Das, S. Xu, L. A. Archer, *Electrochem. Commun.* **2013**, *27*, 59.
[33] P. Hartmann, C. L. Bender, M. Vra ar, A. K. Dürr, A. Garsuch, J. Janek, P. Adelhelm, *Nat. Mater.* **2013**, *12*, 228.
[34] P. Hartmann, C. L. Bender, J. Sann, A. K. Dürr, M. Jansen, J. Janek, P. Adelhelm, *Phys. Chem. Chem. Phys.* **2013**, *15*, 11661.
[35] B. J. Lee, D.-H. Seo, H.-D. Lim, I. Park, K.-Y. Park, J. Kim, K. Kang, *Chem. Mater.* **2014**, *26*, 1048.
[36] S. Kang, Y. Mo, S. P. Ong, G. Ceder, *Nano Lett.* **2014**, *14*, 1016.
[37] T. Ogasawara, A. Débart, M. Holzapfel, P. Novák, P. G. Bruce, *J. Am. Chem. Soc.* **2006**, *128*, 1390.
[38] S. a. Freunberger, Y. Chen, N. E. Drewett, L. J. Hardwick, F. Bardé, P. G. Bruce, *Angew. Chem. Int. Ed.* **2011**, *50*, 8609.
[39] T. Zhang, H. Zhou, *Nat. Commun.* **2013**, *4*, 1817.
[40] B. D. Adams, C. Radtke, R. Black, M. L. Trudeau, K. Zaghib, L. F. Nazar, *Energy Environ. Sci.* **2013**, *6*, 1772.
[41] Y. Li, H. Yadegari, X. Li, M. N. Banis, R. Li, X. Sun, *Chem. Commun.* **2013**, *1*, 10.
[42] H. A. Wriedt, *Bull. Alloy Phase Diagrams* **1987**, *8*, 234.
[43] G. Belov, B. Trusov, *Phys. Chem. Chem. Phys.* **1998**, *102*, 1874.
[44] S. E. Stephanou, W. H. Schechter, W. J. Argersinger, J. Kleinberg, *J. Am. Chem. Soc.* **1949**, *71*, 1819.
[45] K. Chang, B. Hallstedt, *Calphad* **2011**, *35*, 160.
[46] V. S. Bryantsev, M. Blanco, F. Faglioni, *J. Phys. Chem. A* **2010**, *114*, 8165.
[47] R. H. Snow, *U. S. Govt. Res. Dev. Rept* **1966**, *41*, 29.
[48] G. S. Hill, D. G. Holah, S. D. Kinrade, V. R. Magnuson, V. Polyakov, T. A. Sloan, *Can. J. Chem.* **1997**, *75*, 46.
[49] P. Hartmann, D. Grübl, H. Sommer, J. Janek, W. G. Bessler, P. Adelhelm, *J. Phys. Chem. C* **2013**, *118*, 1461.
[50] E. Peled, D. Golodnitsky, R. Hadar, H. Mazor, M. Goor, L. Burstein, *J. Power Sources* **2013**, *244*, 771.
[51] B. D. McCloskey, A. Valery, A. C. Luntz, S. R. Gowda, G. M. Wallraff, J. M. Garcia, T. Mori, L. E. Krupp, *J. Phys. Chem. Lett.* **2013**, 2989.
[52] B. M. Gallant, R. R. Mitchell, D. G. Kwabi, J. Zhou, L. Zuin, C. V. Thompson, Y. Shao-Horn, *J. Phys. Chem. C* **2012**, *116*, 20800.
[53] Z. Peng, S. a. Freunberger, Y. Chen, P. G. Bruce, *Science* **2012**, *337*, 563.
[54] P. Ramadass, B. Haran, R. White, B. N. Popov, *J. Power Sources* **2002**, *111*, 210.